

Molecular Probe Location in Reverse Micelles Determined by NMR Dipolar Interactions

Debbie C. Crans,* Christopher D. Rithner, Bharat Baruah, Bridget L. Gourley,[†] and Nancy E. Levinger*

Contribution from the Department of Chemistry, Colorado State University, Fort Collins, Colorado 80523-1872

Received December 9, 2005; E-mail: debbie.crans@colostate.edu; nancy.levinger@colostate.edu

Abstract: The location and interactions of solutes in microheterogeneous environments, such as reverse micelles, critically influence understanding of many phenomena that utilize probe molecules to characterize properties in chemical, biological, and physical systems. The information gained in such studies depends substantially on the location of the probe used. Often, intuition leads to the assumption that ionic probe molecules reside in the polar water pool of a system. In this work, the location of a charged polar transition metal coordination complex in a reverse micellar system is determined using NMR spectroscopy. Despite the expected Coulomb repulsion between the surfactant headgroups and the negatively charged complex, the complex spends significant time penetrating into the hydrophobic portion of the reverse micellar interface. These results challenge the assumption that ionic probe molecules reside solvated by water in microheterogeneous environments and suggest that probe molecule location be carefully considered before interpreting data from similar systems.

I. Introduction

Spectrally active molecules are frequently utilized as probes of molecular systems. For example, molecules that have different spectra in protonated and ionic forms are often used to gauge the pH of a solution.¹ These molecules can be particularly useful in microheterogeneous systems, especially biological systems, where micro- or nanoscopic features preclude measurements using macroscopic methods. Researchers have used a range of molecules to reveal details about pH,² microviscosity,³ and polarity,⁴ among others, in confined environments, such as cells, micelles, and nanoporous materials. Generally, the molecular probes are chosen for their spectroscopic handles and the ability to interpret the observations made. Experiments utilizing molecular probes of micro- and nanoscopic structures rely on the location of the probe molecule, frequently assuming the location based on a particular feature.^{5–13} A comprehensive review

documents the interpretation that charged molecules reside in the most polar environment available, such as an aqueous phase, while less polar molecules may reside in the micellar interface.⁵ The spectroscopic signatures used to gauge the nature of the local environment are often employed to determine the probe location, but in the research we report here, the expected locations for molecular probes based on charge are not substantiated by our experiments.

In this work, we utilize spin–spin interactions apparent from NMR nuclear Overhauser effect (NOE) experiments to investigate the location of a small oxovanadium complex in microheterogeneous medium. Specifically, we explore a metal complex, dipicolinatodioxovanadium(V) ([VO₂dipic][−]), and its free ligand (dipic^{2−}) and their interactions with the surfactant interface in Aerosol OT (AOT) microemulsions. Structures for these molecules and numbering schemes¹⁴ for their protons are given in Figure 1. The [VO₂dipic][−] complex is well characterized both in the solid state and in solution.^{15,16} In slightly acidic solutions, the complex is very stable and can be studied using multinuclear NMR spectroscopy. Not only is the complex an excellent probe,¹⁷ like other vanadium compounds, it has insulin-like properties and may have biomedical relevance.^{18–20} Thus,

[†] On sabbatical leave. Permanent address: Department of Chemistry, DePauw University, Greencastle, IN 46135.

- (1) Harris, D. C. *Quantitative Chemical Analysis*, 6th ed.; W. H. Freeman and Co.: New York, 2003.
- (2) Caselli, M.; Mangone, A.; Traini, A. *Ann. Chim.* **1998**, *88*, 299.
- (3) Hasegawa, M.; Sugimura, T.; Suzuki, Y.; Shindo, Y.; Kitahara, A. *J. Phys. Chem.* **1994**, *98*, 2120.
- (4) Ueda, M.; Kimura, A.; Wakida, T.; Yoshimura, Y.; Schelly, Z. A. *J. Colloid Interface Sci.* **1994**, *163*, 515.
- (5) Silber, J. J.; Biasutti, A.; Abuin, E.; Lissi, E. *Adv. Colloid Interface Sci.* **1999**, *82*, 189.
- (6) Luisi, P. L.; Giomini, M.; Pileni, M. P.; Robinson, B. H. *Biochim. Biophys. Acta* **1988**, *947*, 209.
- (7) Singh, A. K.; Majumdar, N. *J. Photochem. Photobiol. B: Biol.* **1995**, *30*, 105.
- (8) Hung, H.-C.; Chang, G.-G. *J. Chem. Soc., Perkin Trans.* **1999**, *2*, 2177.
- (9) Lissi, E. A.; Abuin, E. B.; Rubio, M. A.; Ceron, A. *Langmuir* **2000**, *16*, 178.
- (10) Caselli, M.; Daniele, V.; Mangone, A.; Paolillo, P. *J. Colloid Interface Sci.* **2000**, *221*, 173.

- (11) Caselli, M.; Mangone, A.; Paolillo, P.; Traini, A. *Ann. Chim.* **2002**, *92*, 501.
- (12) Gunaseelan, K.; Romsted, L. S.; Gonzalez-Romero, E.; Bravo-Diaz, C. *Langmuir* **2004**, *20*, 3047.
- (13) Sarma, S.; Dutta, R. K. *J. Surfactants Deterg.* **2005**, *8*, 277.
- (14) Ueno, M.; Kishimoto, H.; Kyogoku, Y. *J. Colloid Interface Sci.* **1978**, *63*, 113.
- (15) Nuber, B.; Weiss, J.; Wieghardt, K. *Z. Naturforsch. B* **1978**, *33*, 265.
- (16) Crans, D. C.; Yang, L. Q.; Jakusch, T.; Kiss, T. *Inorg. Chem.* **2000**, *39*, 4409.
- (17) Stover, J.; Rithner, C. D.; Inafuku, R. A.; Crans, D. C.; Levinger, N. E. *Langmuir* **2005**, *21*, 6250.

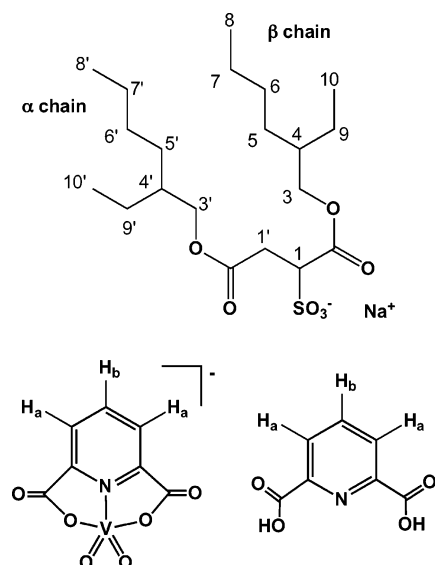


Figure 1. Molecular structure of the AOT molecule (top), $[\text{VO}_2\text{dipic}]^-$ complex (bottom left), and H_2dipic ligand (bottom right).

it is useful to gauge its interaction with self-assembled systems and model membrane systems.

In the $[\text{VO}_2\text{dipic}]^-/\text{water}/\text{AOT}/\text{isooctane}$ system reported here, both the metal complex and the free ligand are highly polar and charged. Intuition and precedent suggest that the charge on these molecules would lead them to reside in the water pools formed in the microemulsion or at the surfactant interface depending on the charge of the surfactant headgroups at the surfactant interface. Indeed, for cationic surfactant headgroups, our previous results suggest that probes experience Coulomb attraction, leading the molecules to reside in the water pool interacting with the cationic headgroups.¹⁷ In contrast, Coulomb repulsion from the anionic sulfonate headgroups of AOT should cause the negatively charged vanadium complex to dive away from the interface toward the water pool. The experiments described here show unequivocally that these polar and charged probes reside buried in the hydrophobic interface region away from the water pool.

It is well accepted that the nuclear Overhauser effect (NOE), a ubiquitous tool of macromolecular structure determination, can be used to measure the spatial proximity of two atoms in a sample.^{21–24} If atoms are close to each other, their spins can interact, transferring population from one NMR signal to another, but the strength of the interaction drops precipitously as the distance increases. This technique has been used exhaustively in structural biology, gauging both intra- and intermolecular distances and interactions.^{21–24} In addition, the sign of the NOE reflects the mobility of a probe. While commonly used for macromolecular structural determination, the NOE can be used to investigate the proximity of any two

protons in a sample, including protons on two different molecules as well as the proximity of protons within a given molecule, as long as the protons are close enough and have sufficient time to interact on the NMR time scale. Bachofer and co-workers have used NMR NOE to gauge the location of small aromatic molecules interacting with micelles in aqueous media.^{25,26} Ceraulo et al. have used NOE to explore the confinement of urea in reverse micelles and found interactions between the urea protons and protons in the AOT headgroup region.²⁷ Kreke et al. used 1- and 2D NMR to show that dichlorobenzoate counterions intercalate among the surfactants' headgroups in CTAB micelles.²⁸ These studies demonstrate the suitability of the NOE technique for probing interactions of molecules in reverse micelles.

In this paper, we report the results from NOE experiments on $[\text{VO}_2\text{dipic}]^-$ in AOT microemulsions. We take advantage of the NOE effect and its sign to measure the interactions of protons on our $[\text{VO}_2\text{dipic}]^-$ complex and the dipic^{2-} ligand with protons on the AOT surfactant that comprises the micellar interface.

II. Materials and Methods

Materials. Ammonium dipicolinatodioxovanadium(V) ($\text{NH}_4[\text{VO}_2\text{dipic}]$) was prepared following procedures in the literature.^{15,16,29} 2,6-Pyridinedicarboxylic acid (H_2dipic) and AOT (sodium bis(2-ethylhexyl)-sulfosuccinate) were purchased from Aldrich. The latter was purified using a standard literature method.³⁰ Deuterium oxide (D_2O) and deuterated 2,2,4-trimethylpentane ($(^2\text{H}_{18})\text{isooctane}$) were obtained from Cambridge Isotope Laboratories Inc. and used as received.

Sample Preparation. The 200 mM stock solution of $\text{NH}_4[\text{VO}_2\text{dipic}]$ was prepared by dissolving the crystalline solid complex volumetrically in D_2O . Similarly, a 200 mM stock solution of 2,6-pyridinedicarboxylic acid was prepared by dissolving the solid in 0.4 M NaOD and then adjusting the pH to 6.0 with DCl before making up the volume in a volumetric flask with D_2O . The pH values of the solutions were measured at 25 °C using an Orion 420A pH meter and were not corrected for the presence of D_2O (± 0.4).

The microemulsions were prepared by dissolving AOT in isooctane under ambient conditions to yield a 1.0 M solution. For NOE experiments, samples were created with perdeuterated isooctane, while 1D ^{51}V NMR studies were performed with protonated solvent. The $\text{NH}_4[\text{VO}_2\text{dipic}]$ or 2,6-pyridinedicarboxylic solutions were added to the AOT stock solution, and the mixtures were vortexed, resulting in clear solutions. Microemulsion samples of lower overall concentration were prepared by dilution of the 1.0 M samples with isooctane. The size of the reverse micelles in solution, gauged by $w_0 = [\text{water}]/[\text{AOT}]$, was adjusted by adding the pH-adjusted complex solutions to the AOT stock solution volumetrically. All results given here were from $w_0 = 12$ samples. On the basis of the concentration of AOT, water, and $[\text{VO}_2\text{dipic}]^-$ complex in the microemulsions and the aggregation number for AOT reverse micelles with $w_0 = 12$,³⁰ we estimate 25 vanadium complexes per micelle. With this many complexes in each reverse micelle, there should still be an ample amount of water available to solvate each complex. For example, even if half the water solvate AOT headgroups and Na^+ counterions, at least 30 water molecules remain to solvate each vanadium complex, allowing for complete solvation.³⁰

(18) Thompson, K. H.; McNeill, J. H.; Orvig, C. *Chem. Rev.* **1999**, *99*, 2561.

(19) Crans, D. C.; Smees, J.; Gaidamauskas, E.; Yang, L. *Chem. Rev.* **2004**, *104*, 849.

(20) Crans, D. C. *J. Inorg. Biochem.* **2000**, *80*, 123.

(21) Neuhaus, D.; Williamson, M. P. *The Nuclear Overhauser Effect in Structural and Conformational Analysis*, 1st ed.; VCH: New York, 1989.

(22) Flynn, P. F.; Wand, A. J. High-resolution nuclear magnetic resonance of encapsulated proteins dissolved in low viscosity fluids. In *Nuclear Magnetic Resonance of Biological Macromolecules*; James, T., Dotsch, V., Schmitz, U., Eds.; Academic Press: New York, 2001; Part B.

(23) Mueller, G. A.; Choy, W. Y.; Yang, D. W.; Forman-Kay, J. D.; Venters, R. A.; Kay, L. E. *J. Mol. Biol.* **2000**, *300*, 197.

(24) Gardner, K. H.; Rosen, M. K.; Kay, L. E. *Biochemistry* **1997**, *36*, 1389.

(25) Bachofer, S. J.; Turbitt, R. M. *J. Colloid Interface Sci.* **1990**, *135*, 325.

(26) Bachofer, S. J.; Simonis, U.; Nowicki, T. A. *J. Phys. Chem.* **1991**, *95*, 480.

(27) Ceraulo, L.; Dormond, E.; Mele, A.; Liveri, V. T. *Colloid Surf. A: Physicochem. Eng. Asp.* **2003**, *218*, 255.

(28) Kreke, P. J.; Magid, L. J.; Gee, J. C. *Langmuir* **1996**, *12*, 699.

(29) Wiegardt, K. *Inorg. Chem.* **1978**, *17*, 57.

(30) Chowdhury, P. K.; Ashby, K. D.; Dutta, A.; Petrich, J. W. *Photochem. Photobiol.* **2000**, *72*, 612.

Because all the solutions measured were clear, they are microemulsions. The nature of these microemulsions was characterized using various measures. All measurements were performed at 25 °C. We have used dynamic light scattering (DynaPro MSTC) to characterize the size and polydispersity of the reverse micelles in 0.2 M AOT solutions. Sizes of particles in these samples were similar to those reported in the literature.³¹ Samples were also characterized by their conductivity using a conductivity meter (Orion 150A) equipped with a glass cell with two rectangular Pt electrodes (15 mm × 10 mm) with cell constant of 0.1. The conductivity cell was calibrated with a standard 100 μS/cm solution. We observed decrease in conductivity from 0.4 to 0.1 μS/cm with a decrease in AOT concentration from 1.0 to 0.1 M. No further drop in conductivity was observed for lower AOT concentrations. Additionally, conductivity values showed no changes whether the [VO₂dipic]⁻ complex is present in solution. The conductivity measurements suggest that some aggregation or flocculation could be occurring in the 1.0 M AOT samples.

NMR Experiments. NMR experiments were performed on 300, 400, and 500 MHz (for proton) Varian NMR spectrometers. The ⁵¹V NMR spectra were generally recorded using a spectral window of 8 kHz, 90° pulse, and an acquisition time of 0.096 s with no relaxation delay at 78.9 MHz. ⁵¹V NMR chemical shifts were referenced against an external sample of VOCl₃. Routine parameters were used for the 1D ¹H NMR experiments. Longitudinal relaxation time (*T*₁) measurements were performed using the inversion–recovery method with a spectral width of 6 kHz and an acquisition time of 2.7 s. HSQC experiments were performed at 400 MHz for proton and 100.6 MHz for carbon by using the standard Varian pulse sequence. Both ¹H and ¹³C chemical shifts were referenced against 3-(trimethylsilyl)propane sulfonic acid sodium salt (DSS) as an external reference.

¹H–¹H NOESY (Proton Proton 2D Nuclear Overhauser Enhancement Correlation Spectroscopy) NMR experiments were performed using a Varian Inova-500 NMR spectrometer using the supplied Varian pulse sequence. The NOESY data were acquired with a 7 kHz window for proton in F2 and F1. The NOESY mixing time, *τ*_{mix}, was varied from 0.017 to 1.0 s in order to obtain an NOE build-up curve. The total recycle time was 2.1 s between transients. The data set consisted of 1K complex points in *t*₂ by 256 complex points in *t*₁ using States-TPPI. Cosine-squared weighting functions were matched to the time domain in both *t*₁ and *t*₂, and the time domains were zero-filled prior to the Fourier transform. The final resolution was 3.5 Hz/pt in F2 and 15 Hz/pt in F1. Spectrometer control and data processing were done using the Varian VNMRJ-1.1D software, both the Solaris and the Macintosh versions.

Computational Methods. AOT⁻, [VO₂dipic]⁻, and AOT⁻/[VO₂dipic]⁻ anions were modeled using both CAChe Worksystem (Mac-Version 4.9.3, Fujitsu) and MacSpartan '02 (V. 1.0.8, Wavefunction). In CAChe, AOT⁻ and [VO₂dipic]⁻ were optimized using molecular mechanics followed by MOPAC. The resulting structures were used to build AOT⁻/[VO₂dipic]⁻ representations; the distances between one or two AOT methyl (H8, H8', H10, or H10') or methylene protons (H5, H5', H6, H6', H7, H7', H9, or H9') and one or two [VO₂dipic]⁻ protons (H_a or H_b) were constrained to lie within 1.0–3.0 Å of each other. These constrained complexes were optimized to find lowest energy conformations. Dynamical simulations using the CAChe dynamics package were also explored. In Spartan, AOT⁻ and [VO₂dipic]⁻ were geometry optimized using a Hartree–Fock (HF) level calculation with a 6-31G* basis set. The 100 lowest energy conformations of AOT⁻ of 2916 possible conformations were found using a semiempirical level calculation and an AM1 force field. A number of AOT⁻/[VO₂dipic]⁻ representations were created, again with distances between one or two AOT methyl (H8, H8', H10, or H10') or methylene protons (H5, H5', H6, H6', H7, H7', H9, or H9') and one or two [VO₂dipic]⁻ protons (H_a or H_b) constrained to lie within 2.0 Å of each other.

(31) De, T.; Maitra, A. *Adv. Colloid Interface Sci.* **1995**, *59*, 95.

Table 1. The ¹H NMR Chemical Shifts and Longitudinal Relaxation Times, *T*₁, for the [VO₂dipic]⁻ Complex, Free dipic²⁻ Ligand, and AOT from AOT Microemulsion Solutions in Isooctane and in Aqueous Solution

	chemical group	δ/ppm	<i>T</i> ₁ /s
[VO ₂ dipic] ⁻ in AOT microemulsions			
H _a		8.51	1.15
H _b		8.85	0.68
[VO ₂ dipic] ⁻ in aqueous solution, pH = 4.5			
H _a		8.22	4.72
H _b		8.56	3.01
free dipic ²⁻ in AOT microemulsions ^a			
H _a and H _b		8.19	1.11
free dipic ²⁻ in aqueous solution, pH = 6.1 ^a			
H _a and H _b		7.92	3.27
Aerosol OT			
H8, H8', H10, H10'		1.14	0.67
H5, H5', H6, H6', H7, H7', H9, H9'		1.54	0.44
H1		4.43	0.64
H1'		3.36	0.40
H3		4.35	0.36
H3'		4.21	0.37
H4, H4'		1.83	0.44

^a Above pH 6, the protons in dipic²⁻ appear as a single peak.¹⁶

III. Results

NMR Characterization of [VO₂dipic]⁻ and AOT. Both [VO₂dipic]⁻ and AOT have been characterized previously by ¹H and ¹³C NMR spectroscopy.^{14,16,32–36} For [VO₂dipic]⁻, the solid-state structure is retained in aqueous solution.¹⁵ The chemical shifts for features observed in the ¹H NMR spectra are tabulated in Table 1. The structures of complex and free ligand, as well as the structure and numbering scheme of AOT,¹⁴ are given in Figure 1. Four distinct chemical shift regions can be identified: the aromatic region from 8 to 9 ppm for the dipic²⁻ ligand and [VO₂dipic]⁻ complex protons (pH ~ 5); the AOT methylene (H5, H5', H6, H6', H7, H7', H9, H9') and methyl (H8, H8', H10, H10') groups from 1 to 2 ppm; and the AOT CH at 1.8 ppm (H4, H4'), and the AOT CH and CH₂ groups adjacent to a negatively charged residues (H1, H1', H3, and H3') from 3.4 to 4.5 ppm. Some of these signals, particularly those adjacent to charges, vary with pH and the specific nature of the sample, so differences can be observed when comparing different samples or even when the same sample is investigated at different times. Unambiguous assignments were made using 2D HSQC and 2D TOCSY and are in general agreement with those reported in the literature.^{14,34–36} Because the vanadium complex is present in such small proportion compared to the surfactant, any change in the ¹H NMR spectrum of AOT is not detectable with addition of the [VO₂dipic]⁻ complex.

The ¹H NMR spectrum for the [VO₂dipic]⁻ complex is pH independent, displaying a doublet at 8.22 ppm (two protons) and a triplet at 8.56 ppm (one proton) as reported previously.¹⁶ When the [VO₂dipic]⁻ complex is placed in the AOT microemulsion, the chemical shifts of its protons change. In our AOT microemulsions with *w*₀ = 12, a doublet is observed at 8.51

(32) Ueno, M.; Kishimoto, H.; Kyogoku, Y. *Bull. Chem. Soc. Jpn.* **1976**, *49*, 1776.

(33) Ueno, M.; Kishimoto, H.; Kyogoku, Y. *Chem. Lett.* **1977**, 599.

(34) Demarco, A.; Menegatti, E.; Luisi, P. L. *J. Biochem. Biophys. Methods* **1986**, *12*, 325.

(35) Yoshino, A.; Okabayashi, H.; Yoshida, T.; Kushida, K. *J. Phys. Chem.* **1996**, *100*, 9592.

(36) Yoshino, A.; Sugiyama, N.; Okabayashi, H.; Taga, K.; Yoshida, T.; Kamo, O. *Colloids Surf.* **1992**, *67*, 67.

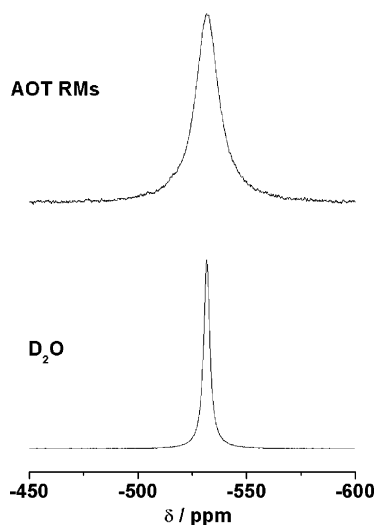


Figure 2. ^{51}V NMR spectrum of $[\text{VO}_2\text{dipic}]^-$ in water/AOT/isoctane microemulsions with $w_0 = 12$ (top) and aqueous solution (bottom). Stock solution of 200 mM $\text{NH}_4[\text{VO}_2\text{dipic}]$ in D_2O , pH = 4.5; microemulsion samples prepared from 1.0 M AOT stock solution in ($^2\text{H}_{18}$)isoctane with the $\text{NH}_4[\text{VO}_2\text{dipic}]$ stock solution at $w_0 = 12$, resulting in an overall concentration of 43 mM $[\text{VO}_2\text{dipic}]^-$.

Table 2. ^{51}V NMR Chemical Shift, Linewidth (Hz), and the Signal Lifetimes (T_2 /ms) for $[\text{VO}_2(\text{dipic})]^-$ Complex in Aqueous Stock Solution and Inside AOT Microemulsions

sample	δ/ppm	line width/Hz	T_2/ms
aqueous stock solution, pH 4.5	-531.5	260	1.3
AOT microemulsions, $w_0 = 12$	-531.5	980	0.5

ppm and a triplet at 8.85 ppm. Similar results are obtained when other values of w_0 are probed.

In addition to its ^1H NMR spectrum, the $[\text{VO}_2\text{dipic}]^-$ complex also displays a ^{51}V NMR spectrum, as shown in Figure 2 and tabulated in Table 2. In aqueous solution, the complex yields a single peak at -531.5 ppm with a 260 Hz linewidth. ^{51}V NMR spectra of AOT reverse micellar samples containing the $[\text{VO}_2\text{dipic}]^-$ complex showed only line broadening but no changes in chemical shift over the range $w_0 = 4\text{--}20$, as shown in Figure 2 for $w_0 = 12$. While linewidths for complexes in the reverse micelles were all broader than those in aqueous solutions, the observed signal linewidths were narrower in larger reverse micelles and increased in smaller reverse micelles. The increasing linewidth reflects a decrease in the transverse relaxation time, T_2^* , which includes contributions from both homogeneous and inhomogeneous broadening mechanisms. We will investigate this issue more thoroughly in the future.

Considering the labile nature of the $[\text{VO}_2\text{dipic}]^-$ complex, it is important to evaluate the free ligand in any analysis of the results. Unlike the $[\text{VO}_2\text{dipic}]^-$ complex, the signals for the free ligand dipic^{2-} depend on pH, reflecting the protonation state of the carboxylate groups.¹⁶ At neutral pH in aqueous solution, the free dipic^{2-} displays a broad signal peaking at 7.92 ppm. In an AOT microemulsion with a $w_0 = 12$, the ^1H NMR peaks appear at a chemical shift of 8.19 ppm. Since the broad signal for the dipic ligand is pH dependent, the observed single peak in the ^1H NMR spectrum demonstrates that the free ligand remains dianionic in the microemulsions. While signals associated with the free ligand do not appear in either ^1H or ^{51}V NMR spectra, they become important for interpreting the NOE data presented below.

To gauge the nature of the microemulsions and our interpretation that these solutions contain isolated water droplets consistent with reverse micelles, we performed several experiments over a range of AOT concentrations. The increased conductivity we observe at higher concentrations (Supporting Information) suggests that the micelles aggregate or flocculate.^{37,38} At the same time, we observed insignificant (0.001 ppm) shifts in ^1H NMR spectra for both surfactant and vanadium complex over the 0.1 to 1.0 M AOT concentration range measured (Supporting Information). No change in chemical shift of the $[\text{VO}_2\text{dipic}]^-$ complex was observed by ^{51}V NMR as the AOT concentration varied (Supporting Information). Changes absent in the NMR spectra suggest that the environments sensed by these molecules remain virtually unchanged. This suggests that some aggregation or flocculation may occur at the high AOT concentrations used for these experiments. The observed ^{51}V NMR signals broadening in solutions of higher AOT concentration is consistent with decreased mobility of the probe observed when micelles aggregate or flocculate.³⁹ These results combined indicate that the immediate environment sensed by the complex is preserved regardless of the aggregation or flocculation of the surfactant concentration that may occur for higher concentrations.

NOE Effects of Solutes in Microemulsion Environments.

$^1\text{H}\text{--}^1\text{H}$ homonuclear NOESY experiments were performed on several reverse micellar samples. Initial experiments on samples using H_{18} -isoctane as the nonpolar phase demonstrated proof of concept, but the superior signal-to-noise ratios of spectra obtained from samples using ($^2\text{H}_{18}$)isoctane are reported here. Figure 3 displays the portion of the NOESY spectrum showing NOEs of the $[\text{VO}_2\text{dipic}]^-$ protons with AOT methylene (e.g., H5, H5', H6, H6', H7, H7', H9, and H9') and methyl groups (e.g., H8, H8', H10, and H10'). The signal-to-noise and chemical shift dispersion of these measurements was insufficient to resolve exactly which of these methylene protons correlate to the vanadium complex. However, what is clear is that the protons closer to the surfactant headgroup and in contact with the reverse micellar water pool (H1, H1', H3, H3') do not display NOE with the $[\text{VO}_2\text{dipic}]^-$ complex at short mixing times, $\tau_{\text{mix}} < 200$ ms. As anticipated in a NOESY experiment, we also observed a series of correlations among the various AOT protons (not shown) that reflect their intramolecular and intermolecular proximity.^{35,36} The intensity of the NOE that we observe between the $[\text{VO}_2\text{dipic}]^-$ complex and the AOT molecules implies that the complex resides in the vicinity of the AOT alkyl tails.

All NOE cross-peaks that we observed are negative. This indicates that the experiments operate at the spin-diffusion limit where $\omega_0\tau_c \gg 1$; ω_0 is the Larmor frequency, and τ_c is the rotational correlation time.²¹ Given that the spectrometer frequency, ν , is 500 MHz means that $\tau_c \gg 300$ ps, substantially longer than the rotational correlation time for an isolated $[\text{VO}_2\text{dipic}]^-$ complex in bulk aqueous solution. The negative correlations associated with intermolecular interactions between $[\text{VO}_2\text{dipic}]^-$ and AOT protons as well as for AOT-AOT NOE cross-peaks correspond to the slow tumbling time of the

(37) Gebicki, J. L.; Gebicka, L. *J. Phys. Chem. B* **1997**, *101*, 10828.

(38) Goto, A.; Kuwahara, Y.; Suzuki, A.; Yoshioka, H.; Goto, R.; Iwamoto, T.; Imae, T. *J. Mol. Liq.* **1997**, *72*, 137.

(39) Andersson, L.; Pettersson, L.; Hastings, J. J.; Howarth, O. W. *J. Chem. Soc., Dalton Trans.* **1996**, 3357.

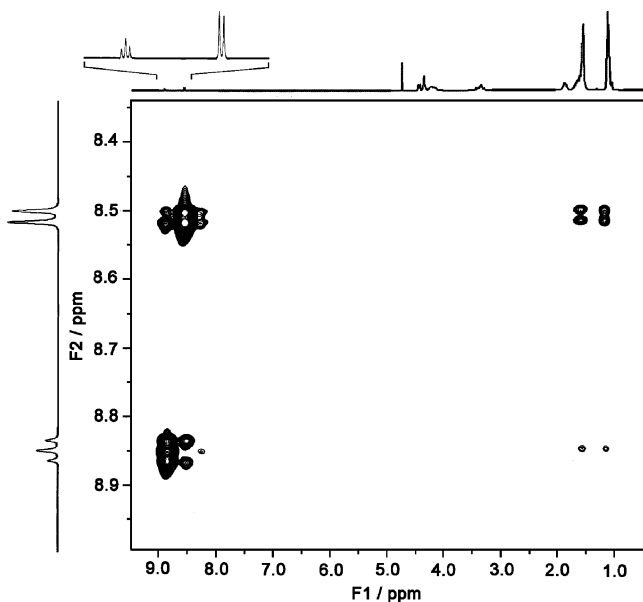


Figure 3. Detail of the NOESY spectrum recorded for the $[\text{VO}_2\text{dipic}]^-$ complex in AOT microemulsions in the region showing the negative NOEs arising from interactions between AOT CH_2 and CH_3 groups and $[\text{VO}_2\text{dipic}]^-$ protons. Note the scale of F2, showing only the dipic ligand protons are substantially expanded compared to F1, which shows the entire range from AOT methyl groups to $[\text{VO}_2\text{dipic}]^-$ protons. Microemulsion samples prepared from 1.0 M AOT stock solution in ($^2\text{H}_{18}$)isooctane with the 200 mM $\text{NH}_4[\text{VO}_2\text{dipic}]$ in D_2O , pH = 4.5 stock solution at $w_0 = 12$, resulting in an overall concentration of 43 mM $[\text{VO}_2\text{dipic}]^-$.

surfactant molecules in their self-assembled configuration.²⁷ Using diffusion coefficients from previously measured pulsed-field gradient NMR experiments¹⁷ of the $[\text{VO}_2\text{dipic}]^-$ complex and the Debye–Stokes–Einstein relation for rotational diffusion, we estimate a lower limit for τ_c of 15 ns and predict that τ_c is actually much longer. In addition, we observe negative NOE cross-peaks corresponding to intramolecular interactions between the meta- and para-protons of the $[\text{VO}_2\text{dipic}]^-$ complex. Because the rotational correlation times for the $[\text{VO}_2\text{dipic}]^-$ complex in aqueous solution should be shorter than 100 ps, the slow rotational correlation time for the $[\text{VO}_2\text{dipic}]^-$ complex evident from these NOE experiments provides further evidence that this complex does not tumble freely and must reside in the reverse micellar interface.

We observe additional intermolecular cross correlations between the $[\text{VO}_2\text{dipic}]^-$ complex and AOT protons for long τ_{mix} because as τ_{mix} increases spin diffusion dominates the NOE signals.²¹ Because it is possible for spin diffusion to dominate

NOESY measurements, we have measured the NOE signal build-up as a function of τ_{mix} . Results are given in Table 3. The trend we observe shows that cross correlation signals between the $[\text{VO}_2\text{dipic}]^-$ complex and AOT methyl and methylene groups beyond the branch point (H5, H5', H6, H6', H7, H7', H8, H8', H9, H9', H10, H10') first rise, then level off or diminish in intensity. For longer τ_{mix} , low intensity NOESY cross-peaks appear at chemical shifts from 1.70 to 4.5 ppm that are not evident for shorter mixing times. These features correspond to cross correlations between the $[\text{VO}_2\text{dipic}]^-$ complex and other AOT protons (e.g., in the headgroup region, H1, H1', α to the carboxylates, H3, H3', and at the alkyl tail branch point, H4, H4'). The delayed rise in these signals demonstrates that spin diffusion accounts for these cross correlations.

Analysis of the NOE data allows us to estimate the proximity of the complex to the surfactant. The NOE intensities depend on the rate and nature of molecular tumbling. In the simplest case, models assume spherical molecules. Using such a model and the intensities of the NOE allows us to gauge the distance between atoms.²¹ We use the intramolecular signals observed for the $[\text{VO}_2\text{dipic}]^-$ complex as a reference from which we can estimate intermolecular distances. In the solid-state structure,¹⁵ the distance between the H_a and H_b protons ranges from 2.294 to 2.296 Å, while the distance between intramolecular meta-protons (H_a and H_α) is 4.021 Å. Given the similarities between structures of the solid state and aqueous $[\text{VO}_2\text{dipic}]^-$ complex, we assume that these distances remain similar in the micelle. It is reasonable to use the $[\text{VO}_2\text{dipic}]^-$ interproton distances to gauge the distances between the $[\text{VO}_2\text{dipic}]^-$ complex protons and the AOT methyl and methylene protons that lead to the observed NOE because both the intramolecular NOESY cross-peaks from the $[\text{VO}_2\text{dipic}]^-$ complex and the intermolecular NOESY cross-peaks from the $[\text{VO}_2\text{dipic}]^-$ complex and AOT are negative. This shows that the complex behaves as a part of the reverse micelle. There are 12 CH_3 protons and 16 CH_2 protons that could contribute to the NOE peaks we see. We model the interactions assuming only half of these protons contribute to the observed NOE intensity. On the basis of this estimation and using the cross correlation NOE intensity, we calculate that the $[\text{VO}_2\text{dipic}]^-$ complex protons H_a and H_b remain within 2.5–4 Å from the AOT CH_2 and CH_3 protons associated with the observed NOE for the duration of one NMR pulse sequence (>1 s). Because the $[\text{VO}_2\text{dipic}]^-$ complex is relatively small compared to AOT, it may have a slightly shorter

Table 3. Negative NOE Signal Buildup as a Function of Mixing Time, τ_{mix} , for NOE Features between Intramolecular $[\text{VO}_2\text{dipic}]^-$ H_a and H_b Protons, and Intermolecular of $[\text{VO}_2\text{dipic}]^-$ H_a and H_b Protons with Various AOT Protons (AOT protons are identified by the chemical shift where they appear. See Table 1 for assignments)

$\tau_{\text{mix}}/\text{s}$	H_a $[\text{VO}_2\text{dipic}]^-/\text{H}_b$ AOT AOT H peak position/ppm ^a						H_b $[\text{VO}_2\text{dipic}]^-/\text{H}_b$ AOT AOT H peak position/ppm ^a				
	8.5	1.2	1.6	1.7 ^b	3.3 ^b	4.4 ^b	1.2	1.6	1.7 ^b	3.3 ^b	4.4 ^b
0.017	0.2	0.0	0.0	0.00	0.00	0.00	0.0	0.0	0.00	0.00	0.00
0.065	0.3	0.1	0.0	0.00	0.00	0.00	0.0	0.0	0.00	0.00	0.00
0.1	0.2	0.2	0.1	0.00	0.00	0.01	0.1	0.0	0.00	0.00	0.00
0.150	1.0	0.2	0.2	0.02	0.01	0.01	0.1	0.1	0.00	0.01	0.00
0.4	1.1	0.4	0.6	0.09	0.04	0.11	0.2	0.2	0.06	0.02	0.03
0.65	1.3	0.5	0.6	0.05	0.03	0.05	0.2	0.2	0.10	0.06	0.12
1	1.7	0.3	0.4	0.07	0.05	0.09	0.1	0.2	0.04	0.02	0.04

^a The peak positions for AOT protons vary slightly from those reported in Table 1 due to sample aging. ^b NOE signals indicated by 0.00 for $[\text{VO}_2\text{dipic}]^-$ H_a and H_b protons with AOT protons appearing at 1.70, 3.34, and 4.40 ppm for short τ_{mix} indicates spin diffusion and does not represent direct correlation between the protons.

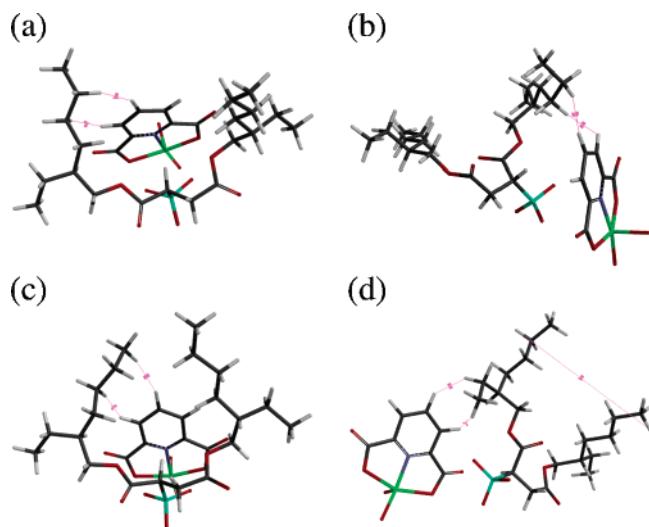


Figure 4. Examples of energetically favorable structures possible for the AOT⁻/[VO₂dipic]⁻ system consistent with the NOE cross-peaks: (a) H_b to H7' and H_a to H6' distances constrained to 2.0 Å, [VO₂dipic]⁻ between AOT alkyl tails; (b) with H_b to H7' and H_a to H6' distances constrained to 2.0 Å, [VO₂dipic]⁻ beside one AOT alkyl tail; (c) with H_a to H6' and H_b to H8' constrained to 2.0 Å; (d) with H_b to H9' and H_a to H10' constrained to 2.0 Å. Calculations were performed using Spartan and represent structures of the AOT⁻ aliphatic tails that should favor self-assembly.

rotational time, and the maximum, negative intramolecular NOESY cross-peak intensity may be less than those expected for interactions of the complex with AOT. This assumption would cause only a slight underestimation of the intermolecular distances between [VO₂dipic]⁻ protons and AOT. While the exact result depends on the assumptions made, an estimation of this type gives a reasonable sense of the distances involved.

We have also developed intuition about the system using molecular modeling. Because the methods available from CAChe or Spartan calculations yield parameters appropriate for gas-phase molecules, we constrained the AOT⁻/[VO₂dipic]⁻ system to configurations that approximate our NOE results and are consistent with self-assembly into the interfacial layer. Although results from these calculations are not quantitative for the microemulsion solution, they can still help to develop intuition about possible interactions that lead to stable structures and facilitate an explanation of the experimental results. Figure 4 shows several selected views of energetically favorable structures for the AOT⁻/[VO₂dipic]⁻ system obtained with our simulation. In Figure 4a and b, the H_b to H7' and H_a to H6' distances are constrained to 2.0 Å, while the AOT aliphatic tails remain in configurations consistent to self-assemble as part of a surfactant interface. Figure 4c shows an energetically favorable structure for the AOT⁻/[VO₂dipic]⁻ system, where H_a to H6' and H_b to H8' distances are constrained to 2.0 Å, while the structure shown in Figure 4d similarly constrains H_b and H_a to H9' and H10', respectively. Amid the vast number of potential conformations, over 3600 per trial, hundreds of potential conformations have energies within 10 kcal/mol of the structures shown. Approximately one-third of those conformations correspond to AOT structures that would allow self-assembly at the boundary between the polar water pool and the nonpolar solvent.

Evidence for Free dipic⁻ Ligand and Chemical Exchange.

In the NOESY spectrum shown in Figure 3, a weak cross-peak appears at 8.2 ppm in the F1 domain. A signal at this chemical

shift does not appear in the 1D ¹H NMR spectrum of [VO₂dipic]⁻ in AOT microemulsions. We attribute this signal to chemical exchange of the [VO₂dipic]⁻ complex with free dipic²⁻ ligand. The [VO₂dipic]⁻ complex is known to exchange with excess ligand in aqueous solution.¹⁶ At neutral pH, free ligand is observed at this chemical shift.¹⁶ Because only a very small quantity of the free ligand exists in solution, we estimate from 0 to 3%, the cross-peak signals for intermolecular interactions, if present, will be even smaller and below our NMR detection limit. The diagonal peak for the free dipic²⁻ ligand is absent in the 2D spectrum because its dephasing time, T₂, is very short and, therefore, not detected. The off diagonal peak appears because it correlates to the more intense [VO₂dipic]⁻ signals. These cross-peaks indicate that chemical exchange occurs frequently between the protons on [VO₂dipic]⁻, the major dipic-containing species, and on the free dipic²⁻ ligand regardless of their location in this complex system. Further experiments on the free ligand are in progress and will be presented elsewhere.

IV. Discussion

The results from these experiments are interesting for several reasons. Chemical intuition introduced in introductory chemistry courses and bolstered by many subsequent examples tells us that a Coulomb interaction between two negative charges should lead to repulsion. Thus, if Coulomb interactions dominate then the negatively charged sulfonate headgroup of the AOT molecules should repel the [VO₂dipic]⁻ complexes, forcing the vanadium complex into the water pool. Indeed, reports in the literature,^{5,6,8,10,13} including our own,¹⁷ echo this view. These reports confirm that small, highly polar and charged solutes should be preferentially solvated in the water pool, while less polar solutes partition into the interfacial region. A variety of studies on nonpolar organic compounds in reverse micelle containing microemulsions show that these molecules reside almost quantitatively in the continuous nonpolar phase.^{5,6} Partition coefficients have been estimated for a large number of molecules with varying polarity and show that the more polar the molecule, the more likely it is to reside in the reverse micellar water pool.^{5,6} In contrast, both the observed NOE and the fact that it is a negative NOE confirm that the negatively charged and highly polar vanadium complex resides buried in the interface.

There exists experimental evidence suggesting that a range of polar and charged molecules can traverse membranes in biological systems.^{40–52} In particular, hydrophobic ions, such as tetraphenylphosphonium cation or tetraphenyl borate anion,

- (40) Ketterer, B.; Neumcke, B.; Lauger, P. *J. Membr. Biol.* **1971**, *5*, 225.
- (41) Andersen, O. S.; Feldberg, S.; Nakadomari, H.; Levy, S.; McLaughlin, S. *Biophys. J.* **1978**, *21*, 35.
- (42) Siddiqi, F. A.; Alvi, N. I.; Khan, S. A. *Colloids Surf.* **1988**, *32*, 57.
- (43) Benz, R. *Ber. Bunsen-Ges. Phys. Chem. Chem. Phys.* **1988**, *92*, 986.
- (44) Schulze, K. D.; Herrnberger, H. Z. *Phys. Chem., Int. J. Res. Phys. Chem. Chem. Phys.* **1995**, *192*, 33.
- (45) Shirai, O.; Yoshida, Y.; Matsui, M.; Maeda, K.; Kihara, S. *Bull. Chem. Soc. Jpn.* **1996**, *69*, 3151.
- (46) Shang, X. M.; Liu, Y.; Yan, E.; Eissenthal, K. B. *J. Phys. Chem. B* **2001**, *105*, 12816.
- (47) Schamberger, J.; Clarke, R. J. *Biophys. J.* **2002**, *82*, 3081.
- (48) Harrigan, P. R.; Hope, M. J.; Redelmeier, T. E.; Cullis, P. R. *Biophys. J.* **1992**, *63*, 1336.
- (49) Franklin, J. C.; Cafiso, D. S.; Flewelling, R. F.; Hubbell, W. L. *Biophys. J.* **1993**, *64*, 642.
- (50) Franklin, J. C.; Cafiso, D. S. *Biophys. J.* **1993**, *65*, 289.
- (51) Madden, T. D.; Redelmeier, T. E. *J. Bioenerg. Biomembr.* **1994**, *26*, 221.
- (52) Franzin, C. M.; MacDonald, P. M. *Biochemistry* **1996**, *35*, 851.

are commonly used to probe potentials across biological membranes. The large hydrophobic groups surrounding the central charged core of these ions lend them solubility in nonpolar environments and allow the ions to traverse the nonpolar part of the interface in a fashion similar to a neutral molecule.^{40,41,47,50,52} In contrast, the $[\text{VO}_2\text{dipic}]^-$ complex used for the studies described here is neither soluble in nonpolar nor soluble in nonaqueous polar solvents. Indeed, the $[\text{VO}_2\text{dipic}]^-$ complex shows its highest solubility in aqueous solutions. Furthermore, studies probing the transit of hydrophobic ions across interfaces all probe bilayers formed from zwitterionic lipids. In our experiments, we use a surfactant with a negatively charged headgroup that should repel the negative charge of the probe complex. Thus, while hydrophobic ions easily pass into and across lipid membranes, we do not expect the same behavior for our $[\text{VO}_2\text{dipic}]^-$ complex interacting with interfaces of AOT reverse micelles.

The results shown here were all for microemulsions $w_0 = 12$, a medium size for AOT reverse micelles. In this medium size, the reverse micelle is large enough ($n_{\text{AOT}} = 129$; $n_{\text{H}_2\text{O}} = 1553$ ³⁰) to accommodate the approximately 25 complexes per reverse micelle without forcing them into the interface. Our previous results^{17,53} and experience have shown that this size provides ample volume in the water pool to completely contain the $[\text{VO}_2\text{dipic}]^-$ complexes in the water phase.

Interestingly, other measures we have applied to gauge the location of the probe molecule, such as ^1H or ^{51}V NMR chemical shifts, suggest less straightforward interpretation of the NOE results. In our ^{51}V NMR experiments, we observe little or no shifting of the ^{51}V NMR peak in the micellar environment or as function of micellar size. At the same time, substantial line broadening indicates reduced mobility of the probe in the local environment. Generally, we interpret broadening and shifting in the ^{51}V NMR spectra to indicate strong interactions, heterogeneity, and altered mobility in the $[\text{VO}_2\text{dipic}]^-$ complexes' environments.¹⁷ The observed broadening suggests reduced mobility, but we would also expect the chemical shift to change when the $[\text{VO}_2\text{dipic}]^-$ complex moved into the nonpolar interfacial region.

The interpretation is less straightforward when considering results for ^1H NMR. Literature reports of ^1H NMR experiments attributed downfield shifts to complex association with the interface, while upfield shifts indicate the complex penetrates the surfactant interface.^{54,55} The ^1H NMR spectrum of the $[\text{VO}_2\text{dipic}]^-$ complex in AOT microemulsions shifts downfield compared to the spectrum in bulk aqueous solution consistent with the complex residing in an aqueous environment at the surfactant interfacial layer rather than penetrating into a more nonpolar region of the self-assembled surfactant layer.^{54,55} In contrast, experiments probing the location of naphthoate anions in alkylammonium surfactant micelles in aqueous solution showed clear evidence for upfield shifting and strong NOE between probe and surfactant, leading the authors to argue that the naphthoate anions are found in the surfactant interfacial layer.²⁶ On the basis of chemical shift arguments, neither our

^1H nor ^{51}V NMR data are completely consistent with our observed NOE results. Although chemical shift data are generally useful in describing molecular environments, further elaboration may be needed, especially when considering complex systems.^{56–59}

We consider a range of possibilities to explain the combined NOE data and the chemical shift data. For example, if the probe were found both in the interface and in the water pool, each population could report on its own environment. To observe the NOE signal, the probe must remain close to the AOT alkyl tails for the duration of one transient, ~ 1 s. It is hard to imagine the probe traversing the extent of the interface to the water pool in a significantly shorter time. If it moves slowly, we would expect to observe NOE cross-peaks with AOT protons other than the methyl and methylene protons beyond the branch point (e.g., H5, H5', H6, H6', H7, H7', H8, H8', H9, H9', H10, and H10'). While we do observe some cross-peaks with H1, H1', H3, H3', H4, and H4' for long mixing times, our NOE buildup experiments confirmed that these arise substantially from spin diffusion rather than from intermolecular interactions. Even though we cannot eliminate this possibility entirely, these considerations challenge the interpretation of dynamic equilibrium for the $[\text{VO}_2\text{dipic}]^-$ complex between the water pool and the hydrophobic interfacial region.

Alternatively, different ensembles of $[\text{VO}_2\text{dipic}]^-$ complexes could exist with some complexes in the interface but most in the water pool. In this case, the effects of the environments would average and the observed chemical shift should reflect the dominating environment. The intermolecular NOE cross-peaks would arise only from molecules in the interface, while other molecules would add to the overall peak position. The overall effect of this would be to reduce the NOE intensity proportional to the partition coefficient of $[\text{VO}_2\text{dipic}]^-$ in the pool compared with it in the interface, leading to an overestimation of the distance between the embedded $[\text{VO}_2\text{dipic}]^-$ and AOT protons in the interface.

Slightly longer longitudinal relaxation times, T_1 , for the $[\text{VO}_2\text{dipic}]^-$ complexes in microemulsions than for the AOT protons is consistent with the AOT molecules experiencing a more restrictive, interacting environment than the $[\text{VO}_2\text{dipic}]^-$ complexes do. Thus, while the $[\text{VO}_2\text{dipic}]^-$ complexes reside in the interfacial region, they may experience somewhat more motional averaging than the surrounding surfactant alkyl tails. Variable rigidity of the AOT alkyl chains could be a source of this differential motion. Reports suggest that one AOT chain is more rigid and shows more restricted motion than the other.^{35,60} It is possible that the $[\text{VO}_2\text{dipic}]^-$ complexes reside largely solvated by more mobile tails, while the T_1 measurements for AOT reflect contributions from mainly dipolar mechanisms. Differences in motion may arise from solvation of both mobile and rigid AOT chains. Since ^1H relaxation is dominated by dipolar interactions, then the relative structural density of the ^1H nuclei in the AOT compared with the $[\text{VO}_2\text{dipic}]^-$ complexes will also play an important role. It will be difficult to separate the motional and structural factors from each other by comparing

(53) Riter, R. E.; Willard, D. M.; Levinger, N. E. *J. Phys. Chem. B* **1998**, *102*, 2705.

(54) Vermathen, M.; Louie, E. A.; Chodosh, A. B.; Ried, S.; Simonis, U. *Langmuir* **2000**, *16*, 210.

(55) Vermathen, M.; Chodosh, A. B.; Louie, E. A.; Simonis, U. *J. Inorg. Biochem.* **1999**, *74*, 328.

(56) Crans, D. C.; Shin, P. K. *J. Am. Chem. Soc.* **1994**, *116*, 1305.

(57) Bodner, M. L.; Gabrys, C. M.; Parkanzky, P. D.; Yang, J.; Duskin, C. A.; Weliky, D. P. *Magn. Reson. Chem.* **2004**, *42*, 187.

(58) Wishart, D. S.; Bigam, C. G.; Yao, J.; Abildgaard, F.; Dyson, H. J.; Oldfield, E.; Markley, J. L.; Sykes, B. D. *J. Biomol. NMR* **1995**, *6*, 135.

(59) Spera, S.; Bax, A. *J. Am. Chem. Soc.* **1991**, *113*, 5490.

(60) Marchi, M. Personal communication, 2005.

only ^1H NMR T_1 . Proton-detected heteronuclear ^{13}C or ^{15}N NOE spectroscopy could be employed to separate these effects and further support this proposal.

The NOE experiments reported here show that the $[\text{VO}_2\text{dipic}]^-$ complex resides buried in the hydrophobic region of the AOT reverse micellar interface. What is not clear is exactly what its environment is. For example, it is possible that the observed NOE could result if an alkyl tail of the AOT were in contact with the $[\text{VO}_2\text{dipic}]^-$ complex in the water pool. Then, it would be possible for the $[\text{VO}_2\text{dipic}]^-$ to be in contact with the alkyl features of the AOT without penetrating the interface. A recent molecular dynamics simulation of AOT reverse micelles with $w_0 = 2$ showed stability for the reverse micelle even when one AOT alkyl chain was in contact with the water pool.⁶¹ Given the low rate of occurrence for AOT hydrophobic carbons dipping into the water layer, this possibility seems unlikely. It is also possible that the $[\text{VO}_2\text{dipic}]^-$ complex drags counterions or water into the interfacial region. This would change the environment near the complex, most likely increasing the local heterogeneity, and therefore should impact the ^1H and ^{51}V NMR spectra. However, with an alkane solvent as the nonpolar continuous phase, it is well documented that water remains sequestered in the micelle interior and does not penetrate into the surfactant interface at all.^{62–64} Indeed, our NMR data are consistent with this interpretation as we saw no cross-peaks between HDO protons and AOT protons.

The appearance of cross-peaks between the $[\text{VO}_2\text{dipic}]^-$ and the free dipic^{2-} ligand in the NMR spectrum is consistent with chemical exchange between the complex and ligand. Chemical exchange has been reported previously for this complex in aqueous solution in the presence of excess free ligand.¹⁶ Because all NOEs reported here are negative, the rotational correlation times are long, which suggests that the dipic^{2-} ligand resides buried in the micellar interface regardless of whether it remains complexed to the vanadium or not. Observation of the dipic^{2-} ligand requires that the complex separates into metal and free ligand components. This can occur either in the water pool or in the interface. For example, the complex could lose a VO_2^+ unit, even though the dipic^{2-} ligand remains deeply buried in the surfactant interface. Such a process would require the VO_2^+ unit to be able to traverse the charged interfacial layer and that the charged free ligand be stabilized in the very hydrophobic environment in the reverse micellar interface. The exchange could also take place when a small fraction of the intact $[\text{VO}_2\text{dipic}]^-$ complex ventures into the water phase. Although the observed chemical exchange in a nonpolar environment is unexpected, our results show that it does take place and suggest that these processes have not been appropriately considered in the past.

Although the complex's shape does not resemble most molecules used as cosurfactants,^{31,65} some features of the $[\text{VO}_2\text{dipic}]^-$ complex may lead it to have this function. It is amphiphilic with both a hydrophobic and hydrophilic regions.

It is elongated and should pack well in an organized self-assembled surfactant structure. In addition, the $[\text{VO}_2\text{dipic}]^-$ possesses a substantial dipole moment. Indeed, on the basis of our HF 6-31G* calculation, the gas phase dipole moment is 14.3 D. Our simulations also show that most of the low energy conformations of the AOT molecule also possess a significant dipole moment. It is possible that dipole–dipole interactions play a key role in determining and stabilizing the ultimate placement for the $[\text{VO}_2\text{dipic}]^-$ complex, even if Coulomb repulsion would favor solvation in the water pool.

Together, all these results challenge the placement of small, charged molecular probes in reverse micellar water pools and have implications for interpretation of data obtained using small molecular probes to characterize complex self-assembled surfactant systems.

V. Summary and Conclusions

This paper presents NMR chemical shift and ^1H – ^1H homonuclear NOE data for $[\text{VO}_2\text{dipic}]^-$ complexes in AOT microemulsions to explore the location of a transition metal complex in a self-assembled system. Both appearance of NOE cross-peaks and the fact that all the NOE signals are negative confirm that this polar and negatively charged complex resides buried in the hydrophobic part of the interfacial region rather than remaining solvated in the water pool. The cross-peaks between protons on AOT alkyl tails and protons on the $[\text{VO}_2\text{dipic}]^-$ complex indicate the close proximity of these two species to each other. The fact that all the observed NOE signals were negative implies that $[\text{VO}_2\text{dipic}]^-$ complex rotational correlation times are far longer than would have been observed if the complex rotated freely in solution and further points to the $[\text{VO}_2\text{dipic}]^-$ complex being embedded in the interface. Straightforward molecular modeling and estimations of intermolecular distances based on our NOE signal intensities enhance interpretations further. These studies also revealed chemical exchange between the $[\text{VO}_2\text{dipic}]^-$ complex with the free dipic^{2-} ligand in a highly unlikely environment. Interpretation of our 1D ^1H and ^{51}V NMR chemical shift changes using the empirical approaches described in the literature is not consistent with the results from the NOE experiments. Our results suggest that caution should be exercised when using chemical shifts alone to draw conclusions that could be impacted by the probe location.

Finding our anionic probe buried in the hydrophobic boundary region of a microemulsion rather than in the water pool is counterintuitive for us and the literature at large.⁵ Our knowledge regarding the interplay between hydrophobic and Coulomb interactions and the molecular properties of the probe (e.g., its insolubility in most nonaqueous systems) and the AOT microemulsion system would guide us to expect this polar negatively charged probe molecule to be solvated by water, in a water pool or at the water/surfactant interface. However, a wide range of factors determine molecular probe location in these complex systems. The results presented here suggest that some fundamental forces or properties other than those commonly considered may dictate the delicate balance determining probe location in specific environments, and assumptions made about the location of molecular probes used in interpreting the characteristics of complex media should be carefully considered.

(61) Abel, S.; Sterpone, F.; Bandyopadhyay, S.; Marchi, M. *J. Phys. Chem. B* **2004**, *108*, 19458.

(62) El Seoud, O. A.; Correa, N. M.; Novaki, L. P. *Langmuir* **2001**, *17*, 1847.

(63) Novaki, L. P.; Correa, N. M.; Silber, J. J.; El Seoud, O. A. *Langmuir* **2000**, *16*, 5573.

(64) Correa, N. M.; Biasutti, M. A.; Silber, J. J. *J. Colloid Interface Sci.* **1995**, *172*, 71.

(65) Chennamsetty, N.; Bock, H.; Scanu, L. F.; Siperstein, F. R.; Gubbins, K. E. *J. Chem. Phys.* **2005**, *122*, 094710.

Acknowledgment. This material is based upon work supported by the National Science Foundation under Grant No. 0314719. B.L.G. gratefully acknowledges DePauw University for partial sabbatical support. The NMR spectrometer used for NOESY experiments was purchased under NIH-SIG RR11981.

Supporting Information Available: Conductivity, ^1H and ^{51}V NMR chemical shift data as function of AOT concentration are provided in Tables S1–S4. This material is available free of charge via the Internet at <http://pubs.acs.org>.

JA0583721